

P-P and As-As isovalent impurity pairs in GaN: Interaction of deep t_2 levels

T. Mattila* and Alex Zunger[†]

National Renewable Energy Laboratory, Golden, Colorado 80401

-Received 9 April 1998!

The electronic and atomic structure of substitutional n th neighbor ($1 < n < 6$) P-P and As-As impurity pairs in zinc blende GaN is investigated using self-consistent plane-wave pseudopotential and empirical pseudopotential methods. A single impurity introduces a deep t_2 gap level; we show that the interaction between the t_2 defect orbitals of the impurity pairs leads to an interesting pattern of single-particle level splitting, being largest for the first ($n=1$) and fourth ($n=4$) neighbor pairs, both exhibiting a

t_2 - t_2 interaction leads to interesting defect level splitting which depends strongly on the pair symmetry and atomic separation. The largest splitting and complete removal of the orbital degeneracy is predicted for $n=1$ and $n=4$ pairs, both exhibiting C_{2v} symmetry, while for $n=2$ with D_{2d} symmetry we find only a partial removal of the degeneracy, and a small splitting.

~iii! The transition probabilities for electronic excitations between the impurity-pair-induced defect levels and the lowest conduction band are found to be large. Since the transitions are energetically well separated from the transitions related to the isolated impurities, the presence of As-As and P-P impurity pairs in GaN should manifest itself via spectroscopic features that are distinct from those of the isolated impurities.

~iv! We calculate the exciton binding energies for nearest neighbor ($n=1$) As-As ~P-P! pairs at $E_b=1.27$ (0.85) eV. These values are considerably larger than those calculated for isolated impurities @ $E_b=0.41$ (0.22) eV for As ~P!#.⁶

~v! Having established the electronic and atomic structure of the impurity pairs we investigate their formation energy $DE^{(n)}$, i.e., the energy of an n th neighbor impurity pair relative to the energy of two isolated impurities ($n \rightarrow \infty$). We decompose $DE^{(n)}$ into two contributions: an elastic part resulting from the long-ranged interaction of the strain fields induced by the two impurities, and a chemical part representing the electronic interactions ~in particular, the interaction induced by the deep t_2 defect orbitals!. We show that both contributions depend strongly on the orientation of the impurity atoms relative to the lattice. We predict P-P and As-As *clustering* at nearest and next-nearest sublattice sites ($DE^{(n)} < 0$, for $n=1,2$), whereas the fourth neighbor configuration is unstable ($DE^{(4)} > 0$). For $n=4$ we find that $DE^{(n)}$ is approaching zero, i.e., weak inter-impurity interaction.

II. METHODS

A. *Ab initio* and empirical pseudopotentials

In this study we will use two approaches, ~i! the *ab initio* and ~ii! the empirical pseudopotential methods, to investigate the atomic and electronic properties of the impurity pairs. With both methods we use supercells to simulate the defect pair placed in an infinite lattice. While an isolated point defect can be reliably studied with moderate size supercells

~typically 64 atoms in the zinc blende structure!, the study of impurity pairs requires the use of larger cells. This can be seen by considering the relative geometries for impurity pairs, representing the n th fcc neighbor ($n=1,2,3,4,5,6$) to each other in the zinc blende structure, described in Fig. 1 and Table I. It is evident that a 64 atom supercell (2 \times 2 \times 2 eight atom unit cells! becomes inadequate when $n=1$. This is due to the periodic boundary conditions which cause the distances between the actual impurity atoms (d_i in Table I! and their periodic images to become equal and thus impose artificial symmetry constraints. Furthermore, we will show below ~Sec. III E! that the strain-mediated impurity-impurity interaction can be long ranged, and can thus require the use of large cells.

As a primary approach in this study we use the self-consistent plane-wave pseudopotential calculations,¹² based on density-functional theory within the local density approximation ~LDA!. The exchange-correlation term is parametrized as by Perdew and Zunger.¹³ For nitrogen we use ultrasoft pseudopotential,¹⁴ while for Ga, As, and P we use norm-conserving pseudopotentials¹⁵ with the nonlinear core-valence exchange-correlation scheme¹⁶ and s component as the local one. The Ga $3d$ orbitals are treated as part of the core.¹⁷⁻¹⁹ A 25 Ry kinetic-energy cutoff is applied for the plane-wave basis, showing excellent convergence of the results with respect to the basis size. In the LDA calculations we use two system sizes: 64 and 216 atom supercells. The use of a 216 atom supercell is enabled by using a highly efficient parallel implementation of the method on the Cray T3E. The Brillouin zone sampling with the 64 atom cell size is done using a 2 \times 2 \times 2 Monkhorst-Pack special k -point grid.²⁰ For the larger 216 atom cell only the G point is used. However, this sampling is accurate with such a large supercell as shown, e.g., in Ref. 21. The alignment of the screened local potential needed to determine the valence band maximum in the LDA defect calculations is done as in Ref. 6. However, when two impurities are present in the 64 atom supercell, the selection of a region inside the supercell where the potential is bulklike becomes difficult due to the influence of the nearby impurities. Therefore, we have approximated the magnitude of the effective potential alignment based on the results for isolated impurities. For the neutral impurity pair we use twice the value found for the corresponding neutral impurity. In the singly positive charge state of the impurity pair ~used for estimation of the exciton bind-

ing energy! we use the isolated values for neutral and singly positive charge states added together. In the LDA calcula-

as follows -i! obtain the relaxed atomic geometries for the $n \in \{1,2,3,4,5,6\}$ impurity pairs using either VFF or LDA methods, -ii! obtain the single-particle level splitting for the deep t_2 orbitals and the transition probabilities into the induced levels using large supercells and EPM, -iii! determine

TABLE V. Bond lengths for GaN:P₂. The relative bond-lengths $R_{\text{Ga-P}}^a/R_{\text{Ga-N}}^0$

impurity-induced atomic displacements ~strain fields! have a long-range character. ~This will be addressed further in Sec. III E!. Qualitatively the atomic relaxations even with the smallest system size ~64 atoms! are consistent with the largest ~13 824 atoms! supercell.

Comparison between LDA and VFF bond lengths for As-As pairs with $n \in \{1, 2, 4, 6\}$ indicates good agreement between the two methods, as discussed already for $n \in \{1\}$ in Sec. II B. We next investigate how the energy level structure reflects these reduced symmetries.

B. Single-particle energy levels and wave functions

An isolated As or P impurity in GaN produces a t_2^6 level inside the gap, occupied by six electrons.⁶ Figures 4 and 5

show the single-particle energy levels of As-As and P-P pairs in GaN as calculated using the EPM. The most prominent fact in Figs. 4 and 5 is that the degenerate t_2 triplet found for the isolated impurities is split for all impurity pairs studied. According to group theory, any l -fold degeneracy bears a one-to-one correspondence to the existence of a l -dimensional irreducible representation of the specific symmetry group.²⁷ Observation of the first column in the character tables of C_{2v} , C_s , and C_2 ~Refs. 27 and 28! shows that for all of these symmetry groups, the irreducible representations are *one* dimensional. This predicts singly-degenerate single-particle levels in the case of $n \in \{1\}$ (C_{2v}), $n \in \{3\}$ (C_s), and $n \in \{5\}$ (C_2) pairs, consistent with the EPM results presented in Figs. 4 and 5. For $n \in \{2\}$ (D_{2d}) and $n \in \{6\}$ (C_{3v})

there is only a partial lifting of the degeneracy, consistent with the two-dimensional representation found in character tables for these symmetry groups.²⁷

The magnitude of level splitting is largest for $n=1$ and $n=4$ pairs with C_{2v} symmetry. The larger interatomic separation for the $n=4$ pair (Table I) reduces the interaction between the t_2 triplets and thus leads to smaller energy level splitting than for the $n=1$ pair. In general, the energy level splitting shows a nonmonotonic behavior as a function of the pair separation d .

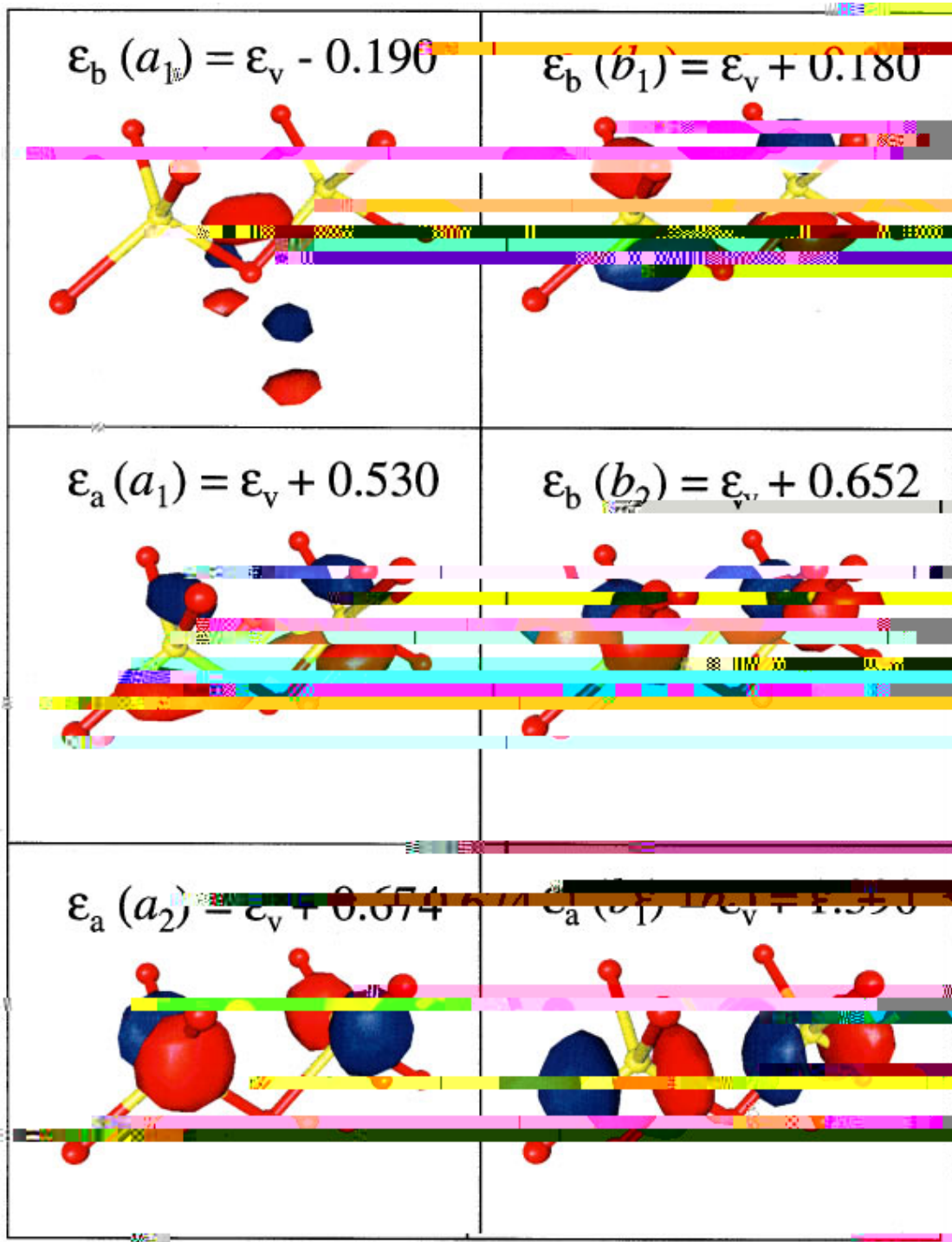


FIG. 6. Color! The wave functions of the impurity orbitals for $n51$ As-As pair. The orbitals correspond to the EPM calculation with 512 atom supercell. The wave functions are illustrated as isosurfaces drawn at approximately half of the maximum amplitude. The red -blue! isosurface corresponds to positive -negative! wave function sign. The yellow -red! atoms correspond to As -Ga! atoms. The subscripts a and b denote antibonding and bonding orbitals, respectively. a_1 , a_2 , b_1 , and b_2 are symmetry representations in C_{2v} -Table VI!.

the transition probabilities between these defect-related split levels and the conduction band. We have thus calculated the -normalized! dipole matrix elements

$$p_a \approx \frac{\langle \psi_{\text{CBM}} | \hat{p} | \psi_a \rangle^2}{\langle \psi_{\text{CBM}} | \hat{p} | \psi_{\text{VBM}} \rangle^2} \quad \sim 1!$$

between the lowest conduction band -from the defect-free bulk calculation! and the defect levels a , normalizing the

values with respect to the direct CBM to VBM transition matrix element in pure GaN. The wave functions are obtained using the EPM and 512 atom supercells. The values for p_a for each n pair are given in Table VII. The dipole matrix for the transition from CBM to defect level of the isolated impurity is 0.05 -0.15 taking the threefold degeneracy into account!. Comparing the values in Table VII with this isolated limit we see that the probability for an electronic transition from the CBM into the highest -single-particle level

$$E_b [E_{\text{gap}} \approx E_{\text{ZPL}}]$$

in the case of $n=1$ and $n=4$ pairs is substantial. Thus we predict that the corresponding emission energies (distinctive from the isolated impurity) should be detectable in photoluminescence experiments for $n=1$ pairs; we show in Sec. III E that $n=4$ pairs are thermodynamically unstable and therefore the experimental verification of their optical character may be more complicated.

D. Exciton binding energy

In Ref. 6 it was shown that the $n=0$ ionization level can be identified as the exciton binding energy:

thermore, due to the low computational cost in VFF calculations, we can investigate the convergence of the elastic energy as a function of system size using large supercells.³⁷

2. The elastic contribution

The elastic contribution $DE_{\text{elast}}^{(n)}$ is shown as dashed lines in Fig. 7. The absolute magnitude of $DE_{\text{elast}}^{(n)}$ converges slowly as a function of the supercell size m ; only the $m \approx 4096$ atom supercell results are nearly indistinguishable from the $m \approx 13824$ atom system. However, the relative energies between different n 's in $DE^{(n)}$ remain nearly identical. The slow convergence of the absolute values with m indicates a long-range interaction of the strain fields induced by the two impurities. This is expected from the classic solution for a spherical inclusion in an isotropic matrix with nonequal lattice parameter:³¹ the elastic displacement decays as a power law \sim the inverse square of the distance from the center of distortion!

$DE_{\text{elast}}^{(n)}$ \sim with the converged system size $m \approx 13824$) is positive for $n \approx 1$ and $n \approx 4$ pairs (C_{2v} symmetry!), indicating repulsive elastic interaction between the impurity atoms at these positions. For $n \approx 2, 3, 5,$ and 6 we find small *negative* values for $DE_{\text{elast}}^{(n)}$ corresponding to attractive interaction between the As atoms. These results are similar to the VFF results for nitrogen impurity pairs in GaAs.²⁶ Thus, the elastic interaction energies would suggest that As-As pairing avoids $n \approx 1$ and $n \approx 4$ neighbor shells and favors $n \approx 2$ and $n \approx 3$ configurations.

3. Chemical contribution

The chemical contribution $DE_{\text{chem}}^{(n)} \approx DE_{\text{LDA}}^{(n)} \approx DE_{\text{elast}}^{(n)}$ plays an important role in determining the pair interaction energy. For consistency, the $m \approx 216$ atom cell size is used both for $DE_{\text{LDA}}^{(n)}$ and $DE_{\text{VFF}}^{(n)}$ when calculating $DE_{\text{chem}}^{(n)}$. In particular, the chemical energy is ≈ 0.23 eV for $n \approx 1$, ≈ 0.13 eV for $n \approx 2$, and small for larger n . In order to understand this we analyze the interaction of the deep t_2 defect orbitals. As explained in Sec. III B and Fig. 4 the t_2 - t_2 interaction leads to large splitting of the defect energy levels. The largest splitting of the triply degenerate gap levels was seen to occur in the case of $n \approx 1$ pair (Fig. 4!), while a smaller splitting occurred for the $n \approx 4$ pair due to larger distance between the impurity atoms. As discussed in Sec. III B and Fig. 4 the lowest orbital has a bonding character while the uppermost orbital is antibonding for both $n \approx 1$ and $n \approx 4$ pairs. The ‘‘center of mass’’ for the bonding-antibonding orbitals of $n \approx 1$ pair can be seen to be considerably *lower* than the position of the deep level of the isolated impurity, while for the $n \approx 4$ pair the corresponding average is only slightly below the isolated value. This indicates that the orbitals for the $n \approx 1$ pair induce a significant bonding contribution while the corresponding effect due to orbitals for the $n \approx 4$ is much smaller. The calculated values for $DE_{\text{chem}}^{(n)}$ above indeed confirm this expectation.

Thus, the calculated values for $DE^{(n)}$ predict that, if we assume a thermal equilibrium during the growth process, the As impurities should favor pairing into $n \approx 1$ and $n \approx 2$ nearest and next-nearest neighbor configurations rather than be evenly \sim randomly! distributed. For P impurity pair we expect

1. Total formation energy

The 216-atom/cell LDA calculated total pair formation energies $DE^{(n)}$ for the As-As pairs are shown as solid line in Fig. 7. The result for $DE^{(n \approx 1)}$ is negative (≈ 0.18 eV). $DE^{(n \approx 2)}$ is slightly higher than $DE^{(n \approx 1)}$, but remains negative indicating binding between the impurity atoms.³⁶ For $DE^{(n \approx 4)}$ we find a large positive value suggesting that the $n \approx 4$ configuration is unstable with respect to dissociation. $DE^{(n \approx 6)}$ is found to have a small negative value indicating only minor interaction between the impurities. Thus, our results predict clear association for $n \approx 1, 2$ and dissociation for $n \approx 4$.

To understand the trends with $DE^{(n)}$ as a function of n and to study the system size dependence we decompose $DE^{(n)}$ into an elastic strain part $DE_{\text{elast}}^{(n)}$, and a chemical part $DE_{\text{chem}}^{(n)}$:

$$DE^{(n)} \approx DE_{\text{elast}}^{(n)} + DE_{\text{chem}}^{(n)}. \quad (5)$$

The self-consistent LDA calculations include both elastic and chemical contribution to the formation energy. The purely elastic strain energy part $DE_{\text{elast}}^{(n)}$ is modeled by the VFF method which, by construction, has only deformation terms, but no charge-transfer or orbital-dependent terms. Thus, $DE_{\text{elast}}^{(n)}$ is given by Eq. (4) with the total energies E corresponding to E_{VFF} . Due to the good agreement between the LDA and VFF bond lengths (Table IV) we can use $DE_{\text{elast}}^{(n)}$ given by VFF to estimate the magnitude of chemical part in LDA calculations as $DE_{\text{chem}}^{(n)} \approx DE_{\text{LDA}}^{(n)} - DE_{\text{VFF}}^{(n)}$. Fur-

a similar behavior based on the analogous single-particle orbital energies and atomic geometries.³⁸

IV. CONCLUSIONS

The self-consistent plane-wave pseudopotential and empirical pseudopotential methods are used to study As-As and P-P substitutional impurity pairs in GaN. The results demonstrate an unconventional interaction between the impurity atoms.

We show that the interaction between localized impurity-induced t_2 triplets leads to a large splitting of the degenerate defect levels, which strongly depends on the orientation of the impurity pair with respect to the lattice. The largest splitting is predicted for the $n=5$ 1 and $n=5$ 4 pairs exhibiting C_{2v} symmetry, while only a small level splitting is found for $n=5$ 2 pairs (D_{2d} symmetry!). The calculated dipole matrix elements for transitions between these defect levels and lowest conduction band predict the existence of rich spectroscopic series associated with the pairing of the impurity atoms. The exciton binding energies for $n=5$ 1 As-As and P-P impurity are calculated to be 1.27 and 0.85 eV which are significantly larger

than the values for isolated impurities -0.41 eV for As and 0.22 eV for P!. These results await experimental confirmation.

It is shown that the interaction of the deep electronic orbitals plays an important role in determining the pair formation energies in addition to the interaction of impurity in-

(< 0.05 eV) and nearly constant decrease in the interaction energy for all impurity pairs due to the shift in $DE_{\text{elast}}^{(n)}$. This shift would not alter the qualitative picture. It is more difficult to estimate the convergence of the chemical interaction $DE_{\text{chem}}^{(n)}$. We have estimated this by comparing results with 64 and 216 atom cells for the isolated As impurity: the energy needed to substitute a N atom with an As atom agrees within 0.05 eV between the two system sizes. This indicates reasonable conver-

gence for the isolated impurity already with 64 atom cell. Based on this observation, we believe that the interaction between the periodic images of the localized orbitals in the case of impurity